

Identification of *RAB3IP* as a Novel Oncogene Related to Ovarian Cancer

Xiaohao Li¹, Qian He¹ and Aiqin He^{1*}

¹Department of Gynecology, The People's Hospital of Tongzhou District, Nantong City, Nantong, Jiangsu, China

²Department of Medicine, Medical College of Nantong University, Nantong, China

³Department of Gynecological Oncology, Nantong University Affiliated Cancer Hospital, Jiangsu, China

Abstract

Objective: The incidence of ovarian cancer ranks third among gynecological malignancies, after cervical cancer and endometrial cancer. However, the mortality rate of ovarian cancer has always been the highest. The pathogenesis of ovarian cancer is not fully understood because the ovary is located deep in the pelvis, the onset of the disease is relatively insidious, and ovarian cancer is usually diagnosed at an advanced stage. The aim of our study was to explore new biomarkers and possible therapeutic targets for ovarian cancer.

Methods: We used public data from the cancer genome atlas The Cancer Genome Atlas (TCGA) and Genotype-Tissue Expression (GTEx) databases to explore the expression level of the *RAB3IP* gene in ovarian cancer patients. At the same time, we analyzed the correlation between the *RAB3IP* gene expression and patient survival, and use ROC curve to predict its clinical efficacy. We validated the level of *RAB3IP* in ovarian cancer tissue using WB and q-PCR. We used cck-8, wound-healing assay and colony formation assay to verify its potential biological function in ovarian cancer. By using molecular docking technology to predict potential drug targets. Pathway enrichment analyses was used to analyze the mechanism of the *RAB3IP* in the occurrence and development of ovarian cancer.

Results: In this study, we found that the expression of *RAB3IP* in ovarian cancer is high by bioinformatics and cell biology and verified it with tissue samples. The promotion of *RAB3IP* on the proliferation and migration of ovarian cancer was confirmed by cck-8, wound-healing assay and colony formation assay, and *RAB3IP*-related genes were enriched for their possible functions, which were believed to be involved in the immune and micro environmental regulation of ovarian cancer to some extent. The expression level of *RAB3IP* is also significantly correlated with the prognosis of ovarian cancer. In addition, we performed drug target prediction of *RAB3IP*, identifying austocystin D and belinostat as potential target drugs that may play a role, and used molecular docking for preliminary validation.

Conclusion: All these results provide preliminary evidence that *RAB3IP* can be used as a new ovarian cancer biomarker to develop new therapeutic targets.

Keywords: Ovarian cancer; *RAB3IP*; Bioinformatics; Biomarkers

Introduction

RAB3IP is a major activator of RAB proteins that can affect intracellular transport processes and cytoskeletal reorganization. *RAB3IP* is important in the growth of malignant cells, it has been found to be up-regulated in malignant tumors and has been suggested to be a tumor-specific marker for some malignancies, such as colorectal cancer, large salivary adenocarcinomas, and gliomas. Recent studies have identified *RAB3IP* as a proto-oncogene and metastasis-associated protein in colorectal, large salivary adenocarcinoma and cervical cancer [1-3]. In human colorectal cancer metastasis, *RAB3IP* was found to be specifically activated by hypomethylation of LINE-1 [3]. Further analysis elucidated the hypomethylated state of the LINE-1 sequence in the promoter region of *RAB3IP*, which correlated with overexpression of *RAB3IP* in matched primary cancer and liver metastasis specimens. LINE-1 accompanied by downstream genes such as *RAB3IP* and *MET* may play an important role in the progression of cancer toward metastasis. In gastric cancer studies, *RAB3IP* has been recognized as a marker of poor prognosis because it significantly enhances cell migration, and this effect is attributed to the involvement of *RAB3IP* in Epithelial-Mesenchymal Transition (EMT) to perform its invasion-promoting function. *In vitro* studies also showed that *RAB3IP* overexpression induced changes in the invasive ability and EMT-like phenotype of gastric cancer cells. In addition, the high expression of *RAB3IP* was attributed to the aberrant activation of *SSX2*, while a significant increase in the invasive ability and motility of cancer cells

was observed [4].

However, the expression and potential functions of *RAB3IP* in ovarian cancer are not yet known. In this study, we demonstrated the role of *RAB3IP* in ovarian cancer tissues and cell lines, revealing the potential significance of *RAB3IP* in participating in ovarian cancer invasion and metastasis.

Materials and Methods

Acquirement of target data

Normal tissue microarrays from the GTEx (<https://xenabrowser.net/datapages/>) database and tumor tissue microarrays from the TCGA (<https://cancergenome.nih.gov/>) database were integrated to analyze the differences in *RAB3IP* expression in 34 tumors. Data corresponding

***Corresponding author:** Dr. Aiqin He, Department of Gynecological Oncology, Nantong University Affiliated Cancer Hospital, Jiangsu, China, E-mail: haq0118@163.com

Received: 13-Feb-2024, Manuscript No. DPO-24-127538; **Editor assigned:** 15-Feb-2024, PreQC No. DPO-24-127538(PQ); **Reviewed:** 29-Feb-2024, QC No. DPO-24-127538; **Revised:** 07-Mar-2024, Manuscript No. DPO-24-127538(R); **Published:** 14-Mar-2024, DOI: 10.4172/2476-2024.9.1.227

Citation: Li X, He, He A (2024) Identification of *RAB3IP* as a Novel Oncogene Related to Ovarian Cancer. *Diagn Pathol Open* 9: 227.

Copyright: © 2024 Li X, et al. This is an open-access article distributed under the terms of the Creative Commons Attribution License, which permits unrestricted use, distribution, and reproduction in any medium, provided the original author and source are credited.

to TCGA for ovarian plasmacytoid cystic adenocarcinoma and corresponding normal tissue data in GTEx were extracted to determine the expression levels of *RAB31P* in adjacent normal and ovarian cancer tissues.

Survival analysis

Overall survival of the *RAB31P* high and low expression groups in ovarian cancer was analyzed using the Kaplan-Meier Plotter (<http://kmpplot.com>).

Sankey diagrams

Sankey diagrams were constructed through the *ggalluvial* package in the R software (4.2.2). The Sankey diagram consists mainly of edges, flows and pivots, where edges represent flowing data, flows represent specific values of the flowing data, and nodes represent different classifications. The width of the edges is shown proportionally to the flow, the wider the edge, the larger the value. The distribution of samples in different subgroups is observed through the Sankey diagram.

ROC curve

The accuracy efficacy of *RAB31P* in predicting the prognosis of ovarian cancer was analyzed by ROC curve. ROC curve can reflect the relationship between sensitivity and specificity. The horizontal coordinate is 1-specificity, the vertical coordinate is sensitivity, the closer the horizontal coordinate is to the zero point, the higher the accuracy, and the farther the vertical coordinate is from the zero point, the better the accuracy. The Area Under Curve (AUC) is used to evaluate the prediction efficacy, and the AUC is usually taken as the value of 0.5~1, and the closer it is to 1, the better the prediction effect is.

Tumor stemness score

Cancer stemness score was obtained according to the One-Class Logistic Regression (OCLR) algorithm constructed by Malta, et al. [5]. RNAseq data and corresponding clinical information of 515 ovarian cancer patients were obtained from the TCGA dataset. The OCLR algorithm was used to calculate the mRNA stemness index (Stemness index, Si). In addition, Spearman correlation was used in this paper to map Si to the range (0, 1) by subtracting the minimum value and dividing by the maximum value. All analysis methods and R packages were implemented using the v4.2.2 version of the R software.

Target gene prediction

Based on differentially expressed genes mined from the Linked Omics (<https://www.linkedomics.org/admin.php>) database, the R packages cluster profiler and *ggplot2* were used for functional enrichment and visualization analysis.

Mutation analysis

Use the cBioPortal (<http://www.cbioportal.org/>) website to learn about the frequency of alterations, mutation types, and copy number aberration results for *RAB31P* in TCGA across all cancer types. Obtain somatic mutation data for ovarian cancer patients from the TCGA dataset. Mutation data were downloaded and extracted using the *maftools* package in R software, and then somatic nuclear mutation data from patients in the high and low gene expression groups were visualized and analyzed.

Immunoassay

The relationship between *RAB31P* expression levels and immune infiltration of all types of cancers in TCGA was explored using TIMER2 (<http://timer.cistrome.org/>). The TIDE algorithm was used to find out the correlation between *RAB31P* expression levels and tumor immune infiltration. p-values and partial correlation core values were obtained by purity-adjusted Spearman rank correlation test. The results were visualized as heatmaps.

Drug target prediction

The Gene Set Cancer Analysis (GSCA) is a knowledge base that integrates multiple chemicals, genes, functional phenotypes, and disease-dependent interactions to help study disease-associated environmental exposures and potential drug mechanisms of action, as well as to provide information on oncology drug response data and genome-sensitive markers. The structures of small molecule compounds are available through the National Library of Medicine online at <https://www.nlm.nih.gov/medline/index.html>. And the interactions between small molecule compounds and genes are simulated by molecular docking computers.

Enrichment analysis

R package GSVA was used to analyze the correlation between genes and pathway scores by selecting the parameter *method="sgsea"* and analyzed by Spearman correlation. *p*<0.05 was considered statistically significant.

miRNA prediction

miRNA prediction was performed based on the miRDB online database, which is used for miRNA target prediction and functional annotation by analyzing miRNA target interactions in high-throughput sequencing experiments. In addition, visual analysis was performed by Cytoscape.

Cell culture

Human epithelial ovarian cancer cells A2780 were purchased from the Cell Resource Center of Shanghai Institutes for Biological Sciences, Chinese Academy of Sciences. All cells were grown in an incubator at 37°C, 5% CO₂.

Western blotting

In this study, cells were lysed in RIPA buffer (#P0013B; Beyotime, Shanghai, China) containing a protease inhibitor (#K1007; APExBIO, Houston, USA) and a phosphatase inhibitor (#K1015; APExBIO) for 20 min at 4°C, and the lysate was centrifuged for 20 min at 4°C at 12,000 rpm/min. Centrifugation was performed for 20 min to obtain the supernatant. Proteins were quantified by BCA assay kit (#P0010S, Beyotime), 5 × loading and 1 × loading were added to ensure the consistency of protein concentration, and protein samples were boiled at 100°C for 5 min to prepare the proteins to be detected. And 20 μg per lane was separated by SDS-PAGE and transferred to PVDF membrane (#IPVH00010, Millipore, USA). Then, the membrane was incubated with *RAB31P* antibody (PA5-96927, ThermoFisher) at 4°C overnight, and on the following day, the PVDF membrane was washed three times with TBST for 5 min each time, incubated with rabbit secondary antibody (A7016, Beyotime) for 2 hr at room temperature, and finally developed using ECL reagent (#180-506, Tanon).

Quantitative Polymerase Chain Reaction (qPCR)

Total RNA was extracted using the TransZol Up Plus RNA kit (Ambion, USA), and cDNA was synthesized using the reverse transcriptase kit (Vazyme, Nanjing, China) in addition, the AceQ qPCR SYBR Green Master Mix kit (Vazyme, Nanjing, China) was used for the qPCR reaction. Meanwhile, the data were normalized to GAPDH mRNA, and the qPCR primers for *RAB31P* were as follows: forward 5'-GTGTCATCTACCGCCACAC-3' and reverse 5'-CCCTCTGAGCTTGCGAGT-3'. Cell Counting Kit-8 (CCK-8) for cell viability assay, cells from different groups were incubated for 2 h according to four different time points 0 h, 24 h, 48 h, 72 h by adding 100 μ L of CCK-8 reagent (Vazyme, Nanjing, China) diluted with RPMI 1640. The results were detected at 450 nm on an enzyme meter and the data were collected.

Wound-healing assay

Different groups of cells were planted in 6-well plates, and when the cells were in the exponential growth period and the cell density reached 80%, a line was drawn in the 6-well plate with a 10- μ L lance tip straight, and the initial image of the cell scratch was collected under the microscope, and then the image was taken for the second time under the same field of view after 24 h.

Cell cloning experiment

Cells from different groups were planted in 6-well plates and incubated in the incubator for 14 days. The cells were fixed with 4% paraformaldehyde for 10 min, stained with crystal violet solution and washed with water. The colonies were photographed and quantified after drying at room temperature.

Statistical analysis

Data were expressed as mean \pm Standard Deviation (SD). Statistical analysis was performed using SPSS 25.0 software, and graphs of difference statistics were plotted using Graphpad Prism 8 software. Differences were detected by independent samples t-test or paired samples test. In addition, overall survival analysis was performed using the Kaplan-Meier method and Log-rank test. $P < 0.05$ was considered statistically significant difference. * indicates $P < 0.05$, ** indicates $P < 0.01$, and *** indicates $P < 0.001$.

Results

High expression of *RAB31P* in ovarian cancer

In order to investigate the role of *RAB31P* in tumors, the mRNA expression levels of *RAB31P* in pan-cancers in the TCGA database were first analyzed by bioinformatics. Not surprisingly, the expression of *RAB31P* was significantly different in each tumor (Figure 1A). To validate the expression of *RAB31P* transcriptome level in ovarian cancer, we compared the mRNA levels of *RAB31P* in 88 normal ovarian samples and 427 ovarian cancer samples using the TCGA-GTEX-OV dataset in the XENA database, and the expression of *RAB31P* in ovarian cancer was much higher than that in the normal control group ($P < 0.001$) (Figure 1B). Subsequently, further by verifying whether the results of clinical samples were consistent with the database, tissue samples from three pairs of ovarian cancer patients were collected, and Western Blot experiments confirmed that the protein expression level of *RAB31P* in

ovarian cancer was higher than that of normal controls (Figure 1C). In addition, significantly high mRNA level of *RAB31P* expression in ovarian cancer was also confirmed by real-time quantitative PCR experiments (Figure 1D).

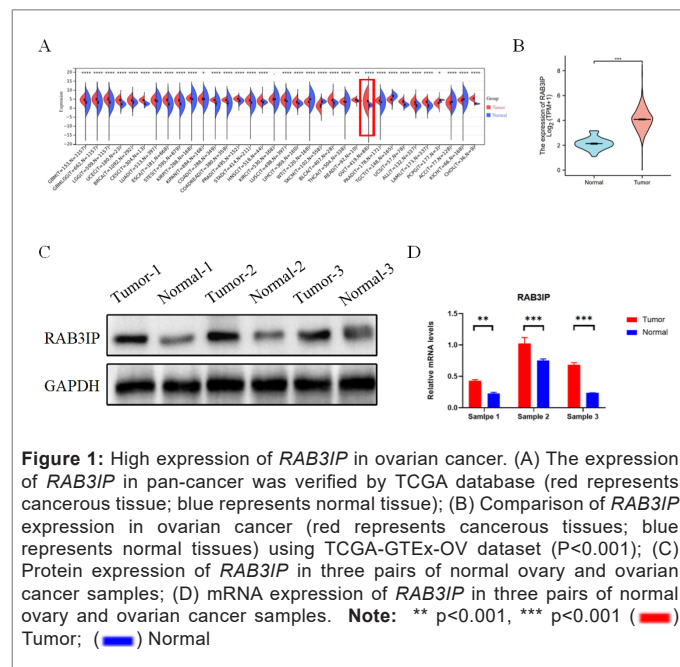
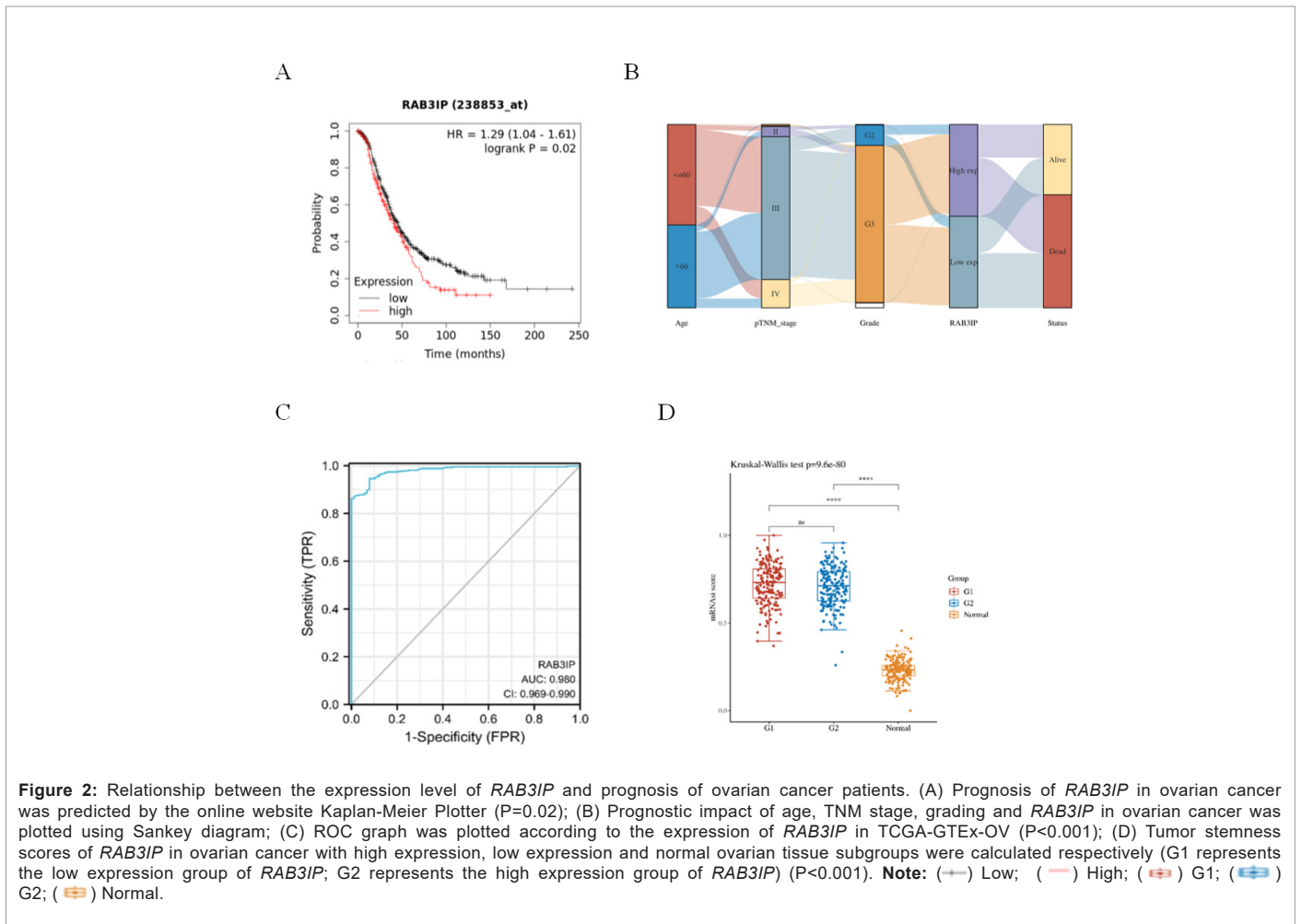


Figure 1: High expression of *RAB31P* in ovarian cancer. (A) The expression of *RAB31P* in pan-cancer was verified by TCGA database (red represents cancerous tissue; blue represents normal tissue); (B) Comparison of *RAB31P* expression in ovarian cancer (red represents cancerous tissues; blue represents normal tissues) using TCGA-GTEX-OV dataset ($P < 0.001$); (C) Protein expression of *RAB31P* in three pairs of normal ovary and ovarian cancer samples; (D) mRNA expression of *RAB31P* in three pairs of normal ovary and ovarian cancer samples. **Note:** ** $p < 0.001$, *** $p < 0.001$ (■) Tumor; (■) Normal

Relationship between the expression level of *RAB31P* and the prognosis of ovarian cancer patients

Based on the above results that *RAB31P* is highly expressed in ovarian cancer, we hypothesized that *RAB31P* promotes the progression of ovarian cancer and is closely related to the prognosis of ovarian cancer patients. Thus, the effect of *RAB31P* on the overall survival of ovarian cancer patients in the TCGA database was analyzed, and the results suggested that ovarian cancer patients with high expression of *RAB31P* had a shorter overall survival (HR=1.29, 95% CI=1.04-1.61, $P=0.02$) and poorer prognosis than those with low expression (Figure 2A). Immediately after that, based on the TCGA dataset to obtain the RNAseq data and corresponding clinical information of ovarian cancer, the distribution trend of age, TNM stage, grade, high and low expression of *RAB31P*, and patient's life and death status in ovarian cancer samples was demonstrated by Sankey diagram, and the results suggested that the branch width of high expression of *RAB31P* had more data flow volume tending to the patient's death status (Figure 2B), which suggests that the patients with high expression of *RAB31P* had a poorer prognosis. The ROC plot is a curve reflecting the relationship between sensitivity and specificity, by which we verified the prognostic ability of *RAB31P* in the TCGA-GTEX-OV cohort, and the AUC area of *RAB31P* was 0.980 ($P < 0.001$) (Figure 2C). Cancer progression involves the progressive loss of differentiated phenotype and the acquisition of stem cell-like features; therefore, we demonstrated that the *RAB31P* high-expression group had better tumor stem cell features compared to the normal control group by calculating the Tumor Stemness Score ($P < 0.001$).



Malignant biological behavior of *RAB31P* in ovarian cancer

In view of the high expression of *RAB31P* in ovarian cancer and its impact on the prognosis of ovarian cancer patients, we further explored its effect on the biological behavior of ovarian cancer cells. First, lentiviral *siRAB31P* was transfected in ovarian cancer cells A2780 for knockdown, and the knockdown efficiency of *RAB31P* was verified by Western Blot experiments, as shown in Figure 3A, the knockdown lentivirus of *RAB31P* demonstrated effective interference efficiency. To further investigate whether *RAB31P* had any effect on the proliferation and migration of ovarian cancer cells, cell survival viability was detected by CCK-8 assay, and the results showed that ovarian cancer cells A2780 with *siRAB31P* could significantly inhibit cell viability with a significant temporal trend at the three time points of 24 h, 48 h, and 72 h, as compared with the control cells (Figure 3B) ($P<0.05$). The 24 h cell migration area was compared by cell scratch assay, and it was found that the *siRAB31P* group was able to significantly inhibit the rate of cell migration (Figure 3C). Consistent with the above results, the number of A2780 cell colonies in the *siRAB31P* group was significantly reduced compared with that in the control group (Figure 3D), and the above results indicated that *RAB31P* was obviously able to promote the proliferation and migration of ovarian cancer cells.

Exploring genes associated with *RAB31P* in ovarian cancer

The Linked Omics database was used to assess the genes associated

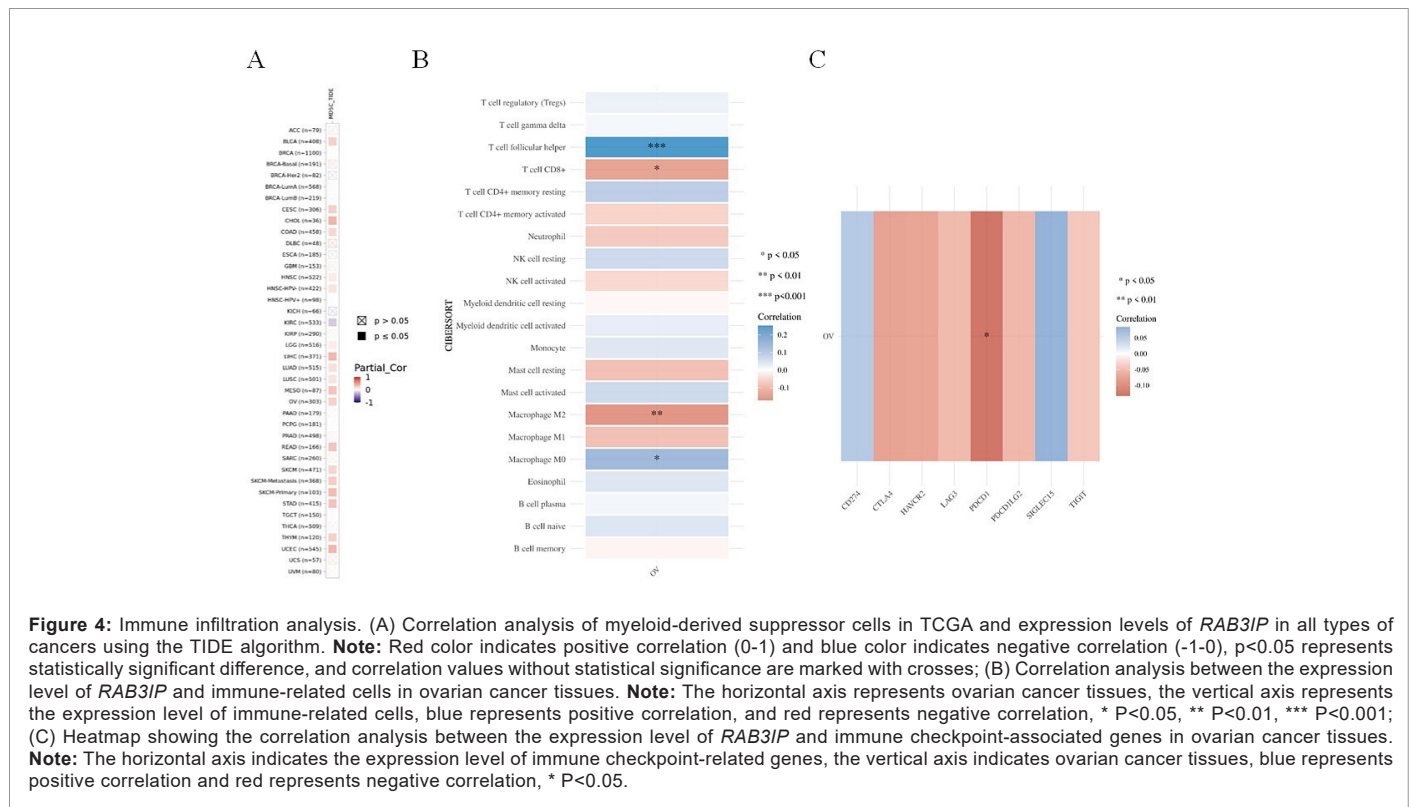
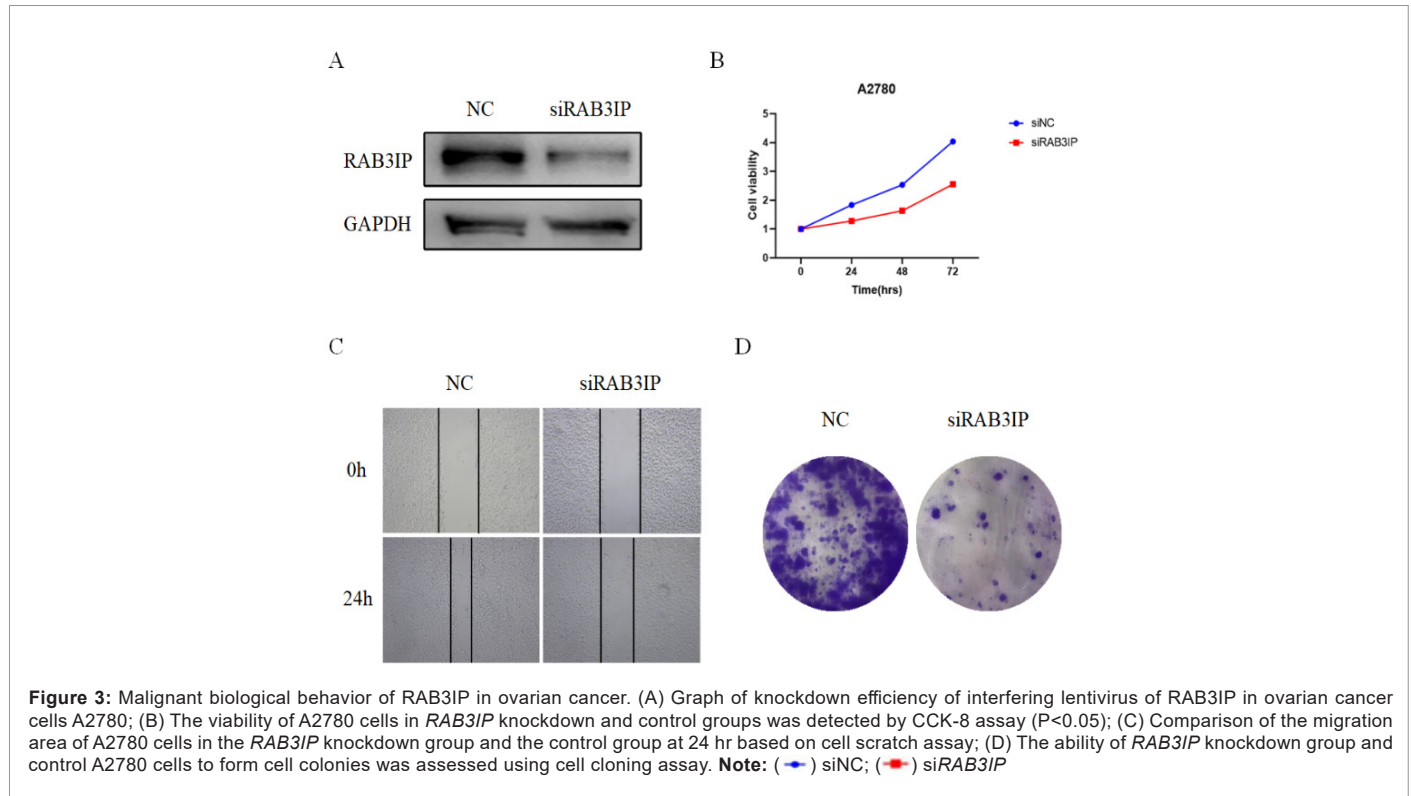
with *RAB31P* in ovarian cancer. The volcano plot in Figure 4A shows that genes positively associated with *RAB31P* are clustered on the right side of the 0.0 value of the abscissa, while genes negatively associated with it are clustered on the left side. The heatmaps of Figures 4B and 4C show the top 50 positively and negatively correlated genes extracted and analyzed according to the Spearman test. In addition, these positively and negatively correlated genes were analyzed for two-by-two correlation in ovarian cancer, respectively, and visualized by heatmaps (Figures 4A and 4C). Immediately after that, the above 100 correlated genes were included in the GO and KEGG pathway enrichment analysis, and it was found that these 100 correlated genes were closely associated with nuclear membrane, nuclear chromatin, mitophagy and cell cycle progression (Figures 4A-4C).

The genetic alterations of *RAB31P* in TCGA

We explored the genetic changes of *RAB31P* in ovarian cancer through cBioPortal based on the TCGA cohort. As shown in Figure 5A, the frequency of *RAB31P* changes in ovarian cancer was higher than 4% compared to various tumors. Moreover, the majority of *RAB31P* alteration frequencies in ovarian cancer were of the "amplification" type, followed by the "mutation" type, and a small number of "multiple variants". Figure 5B shows the types and locations of mutations in the *RAB31P* gene. Based on the mutation map, ovarian cancer patients in the TCGA cohort were categorized into high and low expression groups

according to the median expression value of *RAB3IP*. In the *RAB3IP* high-expression group, the *RYR2*, *CMYA5*, *ABCA1*, *PAPPA2*, and *LAMC1* genes were more inclined to be mutated, whereas in the

RAB3IP low-expression group, significant mutations were observed in the *RYR2*, *NF1*, *ATRX*, *NLRP3*, and *VPS13B* genes (Figures 5A-5E).



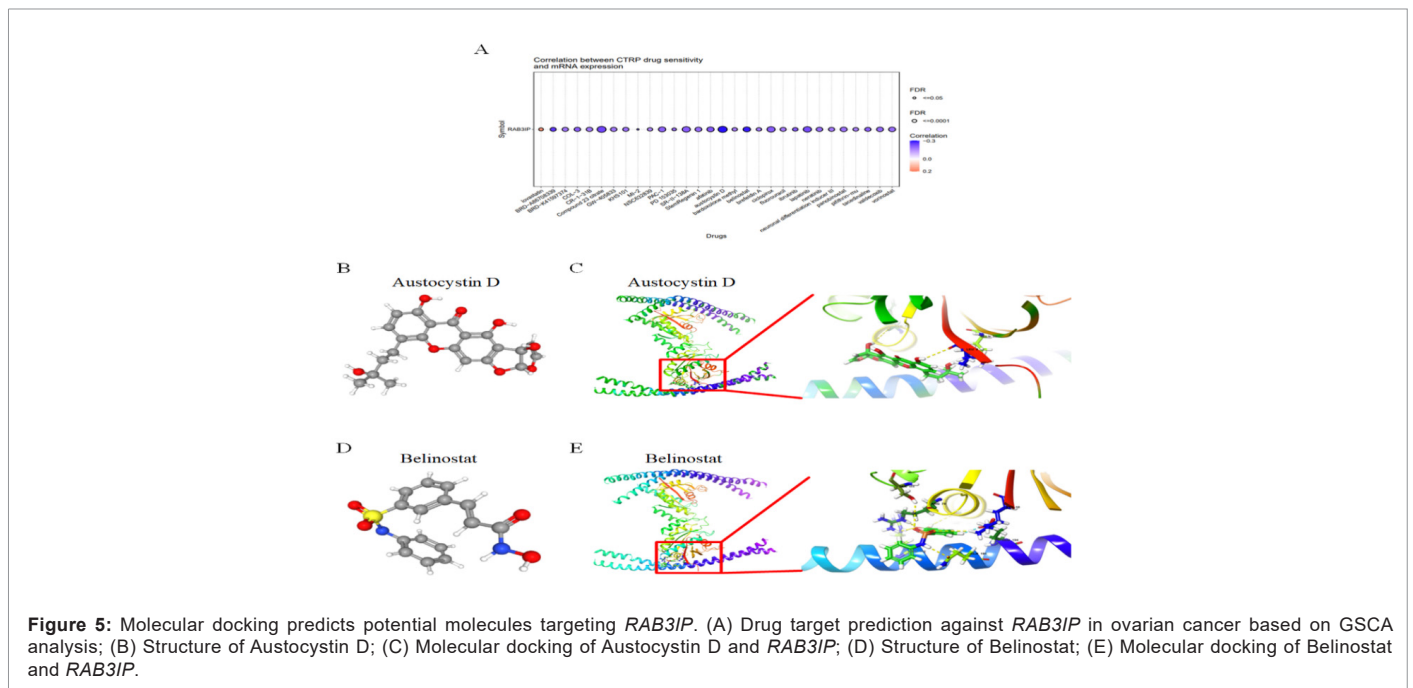


Figure 5: Molecular docking predicts potential molecules targeting *RAB31P*. (A) Drug target prediction against *RAB31P* in ovarian cancer based on GSCA analysis; (B) Structure of Austocystin D; (C) Molecular docking of Austocystin D and *RAB31P*; (D) Structure of Belinostat; (E) Molecular docking of Belinostat and *RAB31P*.

Immune infiltration analysis

Myeloid-derived suppressor cells are a heterogeneous population of immature myeloid cells with immunosuppressive activity (it blocks the proliferation and activity of T cells and natural killer cells). In addition to their role in suppressing immune responses, myeloid-derived suppressor cells directly stimulate tumor cell proliferation, metastasis, and angiogenesis [6]. Therefore, we used TIDE in TIMER2 to explore the correlation between the level of myeloid-derived suppressor cell infiltration and the level of *RAB31P* expression in multiple types of cancers. Importantly, we found that the expression level of *RAB31P* was positively correlated with the infiltration of myeloid-derived suppressor cells and negatively correlated with KIRC in CHOL, LIHC, MESO, OV, and UCEC cancer types (Figure 6A). According to the immune correlation analysis, in ovarian cancer, the expression level of *RAB31P* was positively correlated with follicular helper T cells ($P < 0.001$) and M0 macrophages ($P < 0.05$) and negatively correlated with CD8-positive T cells ($P < 0.05$) and M2 macrophages ($P < 0.01$) (Figure 6B). Immune checkpoint-related genes have attracted the attention of scholars in cancer therapy. Therefore, we explored the correlation between the expression levels of *RAB31P* and the expression levels of immune checkpoint-related genes by co-expression analysis. We found that in ovarian cancer, the expression level of *RAB31P* was negatively correlated with that of the immune checkpoint-related gene PDCD1 ($P < 0.05$) (Figure 6C).

Molecular docking predicts potential molecules targeting *RAB31P*

With the above results we demonstrated the pro-carcinogenic role of *RAB31P* in ovarian cancer, and immediately after, in order to explore molecular compounds that could be used as targeting *RAB31P*, we analyzed the drug sensitivity of *RAB31P*. The two molecular compounds most relevant to *RAB31P* were selected, and Austocystin D and Belinostat were identified as potential targeting agents that could

play a role (Figure 7A). And based on Spearman correlation analysis, the structures of the potential target drugs were identified (Figures 7B-7D). To further validate the binding activity of *RAB31P* and these two drugs, we predicted whether the small molecules had the potential to become drug candidates by computer simulation of molecular docking, and the results showed that both Austocystin D and Belinostat could interact with *RAB31P* (Figures 7C-7D).

Single-sample gene enrichment analysis

Using the collection of genes contained in the relevant pathways in the TCGA database, the enrichment scores of each sample on each pathway were sequentially calculated according to the single-sample gene enrichment analysis algorithm, so as to obtain the connection between the samples and the pathways, and by calculating the correlation between the gene expression and the pathway scores, the relationship between the gene and the pathway can be obtained. Based on this, we found that in ovarian cancer, the expression level of *RAB31P* was positively correlated with the PI3K-AKT-mTOR pathway, tumor proliferation signature, G2M checkpoints, MYC targets, DNA replication, and TGF- β ($P < 0.05$) (Figure 8), whereas it was negatively correlated with the genes up-regulated by reactive oxygen species (ROS), ECM-related genes, tumor inflammation signature, and inflammatory response ($P < 0.05$).

Prediction of miRNAs regulating *RAB31P*

MiRNAs are small non-coding RNAs, typically 18-25 nucleotides long that inhibit protein translation by binding to complementary target mRNAs. miRNAs regulate many biological processes, including cell cycle regulation, cell growth, proliferation, differentiation, apoptosis, metabolism, neuronal patterns, and aging [7]. In this study, we also predicted 224 miRNAs that may target *RAB31P* (Figure 10). It can provide information about miRNAs as biomarkers and therapeutic targets in ovarian cancer.

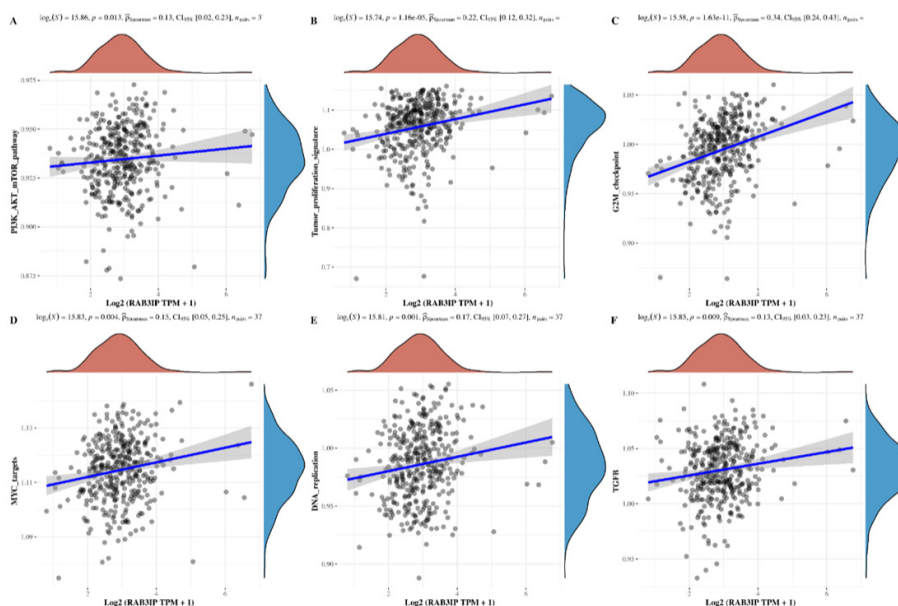


Figure 6: Single-sample gene enrichment analysis. (A-F) The expression level of *RAB3IP* in ovarian cancer was positively correlated with the PI3K-AKT-mTOR pathway, tumor proliferation signature, G2M checkpoints, MYC targets, DNA replication, and TGF- β ($P < 0.05$).

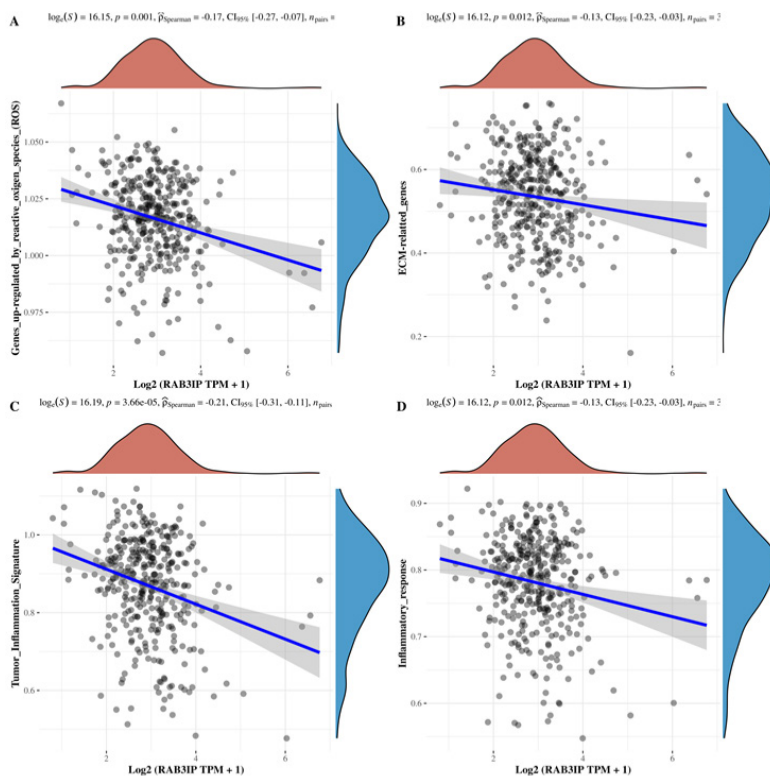


Figure 7: Single-sample gene enrichment analysis. (A-D) The expression level of *RAB3IP* in ovarian cancer was negatively correlated with the genes up-regulated by reactive oxygen species(ROS), ECM-related genes, tumor inflammation signature, and inflammatory response ($P < 0.05$).

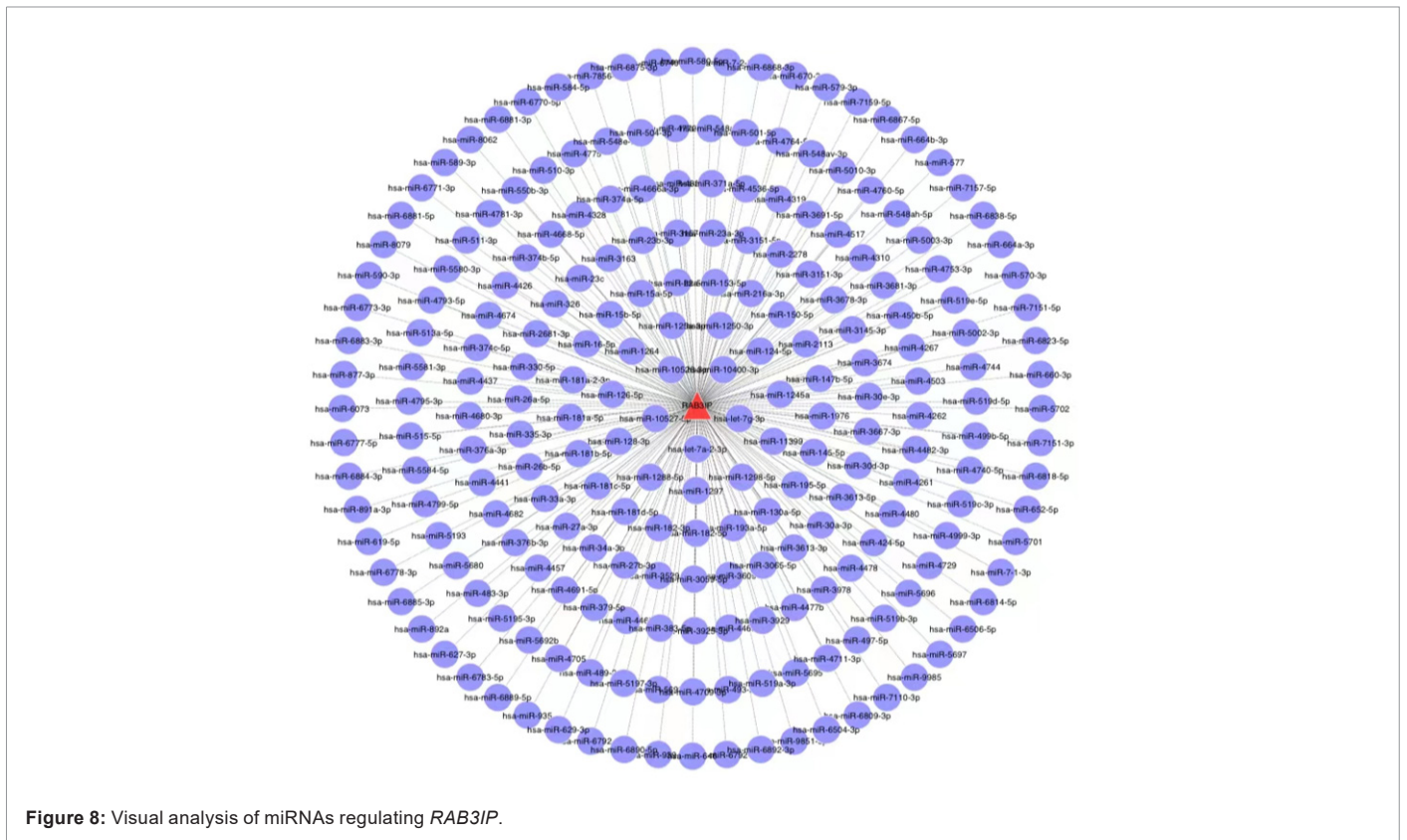


Figure 8: Visual analysis of miRNAs regulating *RAB3IP*.

Discussion

Ovarian cancer is a fatal gynecological cancer with diverse biology at the molecular, cellular and clinical levels [8]. It is the eighth most common cause of death leading to 140,000 women’s deaths [9]. It has the worst prognosis and high mortality rate due to lack of proper screening, poor diagnosis and late detection of the disease, hence it has been called the "silent killer" [10]. Most women diagnosed at advanced stages have a 5-year survival rate of only 46% after standard treatment [11]. CA125 is a useful biomarker for detecting the progression of ovarian cancer, but it lacks sensitivity and specificity because it is increased in benign conditions, such as ovarian cysts, uterine fibroids, and infections [12]. Therefore, there is a need to identify new biomarkers to screen for ovarian cancer.

Comprehensive bioinformatics analysis of microarray data is a powerful tool for analyzing gene expression, protein function, and signaling pathways under various physiological and pathological conditions [13]. It provides a new approach to explore disease-associated genes and predict new molecular interactions, key regulatory molecules, and therapeutic drug targets [14]. Recent studies using bioinformatics analysis based on the TCGA database demonstrated that pyroptosis plays a non-negligible role in the prognostic value, clinicopathological features, and tumor immune infiltration microenvironment of ovarian cancer, which provides new insights into identifying and characterizing the tumor immune microenvironmental landscape, thus guiding a more effective assessment of the prognosis and tailoring of immunotherapeutic strategies for ovarian cancer [15]. However, public databases of extensive genetic profiling data from ovarian cancer patients have not been thoroughly analyzed. *RAB3IP*, a newly discovered member of the RAB protein family in recent years,

acts as an activator protein of the RAB proteins, which is involved in the disease mainly by affecting intracellular transport processes and cytoskeletal remodeling. *RAB3IP* is closely associated with cancer development and disease progression, and it has been suggested that *RAB3IP* may play an important role in malignant cell growth, as it was found to be upregulated and considered as a tumor-specific marker for some malignant tumors (e.g., colorectal cancer, macroosomal adenocarcinoma and gliomas) [1-3]. In this study, the expression of *RAB3IP* in ovarian cancer tissues was detected for the first time by Western Blot and qPCR experiments, and the results showed that the expression of *RAB3IP* in ovarian cancer tissues was significantly higher than that in normal controls, suggesting that the high expression of *RAB3IP* may be involved in the development of ovarian cancer. The role of RAB in tumors has not been well studied, and some researchers have suggested that the regulatory effect of *RAB3IP* on vesicle transport may be through natural immune regulation and thus affect tumor progression [16]. In addition, RAB proteins promote signaling between tumor cells and stromal cells, providing a favorable microenvironment for tumor cell proliferation and invasion [17].

The interaction between *RAB3IP* and *SSX2* was confirmed by de Bruijn, et al. In their study, the co-localization of these two proteins in the nucleus was observed, revealing for the first time that *RAB3IP* is a protein that interacts with *SSX2*. In addition, the interaction between these two molecules was revealed by glutathione chain transferase pull-down assay, which determined that they were co-expressed [18]. *SSX2* is a cancer-associated protein that interacts with *RAB3IP*, which was also found to enhance the invasiveness of breast cancer cells by inhibiting Era signaling [19]. In gastric cancer studies, *RAB3IP* has been recognized as a marker of poor prognosis because it significantly enhances cell migration, and this effect has been attributed to the

involvement of *RAB3IP* in EMT to perform its invasion-promoting function. *In vitro* studies also showed that *RAB3IP* overexpression induced changes in the invasive capacity and EMT-like phenotype of gastric cancer cells. In addition, the high expression of *RAB3IP* was attributed to the aberrant activation of *SSX2*, while a significant increase in the invasive ability and motility of cancer cells was observed [4]. In this study, we further analyzed the relationship between *RAB3IP* expression and the survival prognosis of ovarian cancer patients, and the results showed that *RAB3IP* expression was an independent risk factor affecting the overall survival of ovarian cancer patients, and the overall survival time of ovarian cancer patients with high expression of *RAB3IP* was significantly shorter, which indicated that the expression of *RAB3IP* could be used as an evaluation index for the survival prognosis of ovarian cancer patients.

In this study, *RAB3IP* was knocked down for the first time using siRNA in ovarian cancer cells A2780, and it was found that silencing of *RAB3IP* significantly inhibited the viability, proliferation and migration ability of ovarian cancer cells A2780 ($P < 0.05$). It further indicated that *RAB3IP* was involved in ovarian cancer progression.

In addition, bioinformatics analysis was performed to screen 50 genes positively and negatively associated with *RAB3IP* in ovarian cancer, and found that these 100 genes were closely associated with the nuclear membrane, nuclear chromatin, mitophagy, and cell cycle progression. The frequency of *RAB3IP* alterations was high, and most of the alterations were of the "amplification" type; in the group with high *RAB3IP* expression, *RAB3IP* was highly expressed. In the *RAB3IP* high-expression group, *RYR2*, *CMYA5*, *ABCA1*, *PAPPA2*, and *LAMC1* genes were more likely to be mutated, while in the *RAB3IP* low-expression group, significant mutations were observed in *RYR2*, *NF1*, *ATRX*, *NLRP3*, and *VPS13B* genes. According to the immune correlation analysis, the expression level of *RAB3IP* was positively correlated with the infiltration of myeloid-derived suppressor cells, follicular helper T cells, and M0 macrophages ($P < 0.05$), whereas it was negatively correlated with *KIRC*, CD8-positive T cells, and M2 macrophages ($P < 0.05$). In addition, in ovarian cancer, the expression level of *RAB3IP* was negatively correlated with that of the immune checkpoint-related gene *PDCD1* ($P < 0.05$). Molecular docking was simulated by computer and predicted that Austocystin D and Belinostat could be used as drugs targeting *RAB3IP* in ovarian cancer. By single-sample gene enrichment analysis, the expression level of *RAB3IP* in ovarian cancer was positively correlated with the PI3K-AKT-mTOR pathway, tumor proliferation signature, G2M checkpoints, *MYC* targets, DNA replication, and TGF- β ($P < 0.05$); and negatively correlated with the genes up-regulated by Reactive Oxygen Species (ROS), ECM-related genes, tumor inflammation signature, and inflammatory response ($P < 0.05$). Finally, we predicted 224 miRNAs that might target *RAB3IP*. However, there are still some unanswered questions in this study, such as what is the specific mechanism by which *RAB3IP* promotes ovarian cancer progression, and what genes regulate *RAB3IP* to exert its pro-cancer effects. We will continue to explore these questions in depth in the next step.

Conclusion

Overall, in the present study, we demonstrated that *RAB3IP* is highly expressed in ovarian cancer and promotes ovarian cancer progression, which is positively correlated with the proliferation and migration of ovarian cancer cells. The high expression of *RAB3IP* is significantly associated with poor prognosis of ovarian cancer patients, and it can be used as a new biomarker for ovarian cancer prognosis.

Statements and Declarations

Funding

This work was supported by Nantong Science and Technology Bureau (MS22022007).

Competing interests

The authors have no relevant financial or non-financial interests to disclose.

Author contributions

All authors contributed to the study conception and design. Material preparation, data collection and analysis were performed by Xiaohao Li. The first draft of the manuscript was written by Qian He. Ai Qin He conducted supervision and quality control. All authors commented on previous versions of the manuscript. All authors read and approved the final manuscript.

Data availability

The datasets generated during and/or analysed during the current study are available from the corresponding author on reasonable request.

References

- Fischer U, Keller A, Leidinger P, Deutscher S, Heisel S, et al. (2008) A different view on DNA amplifications indicates frequent, highly complex, and stable amplicons on 12q13-21 in glioma. *Mol Cancer Res* 6:576-84.
- Zhang L, Mitani Y, Caulin C, Rao PH, Kies MS, et al. (2013) Detailed genome-wide SNP analysis of major salivary carcinomas localizes subtype-specific chromosome sites and oncogenes of potential clinical significance. *Am J Pathol* 182:2048-57.
- Hur K, Cejas P, Feliu J, Moreno-Rubio J, Burgos E, et al. (2014) Hypomethylation of long interspersed nuclear element-1 (LINE-1) leads to activation of proto-oncogenes in human colorectal cancer metastasis. *Gut* 3:635-46.
- Ren H, Xu Z, Guo W, Deng Z, Yu X (2018) *Rab3IP* interacts with *SSX2* and enhances the invasiveness of gastric cancer cells. *Biochem Biophys Res Commun* 503:2563-2568.
- Malta TM, Sokolov A, Gentles AJ, Burzykowski T, Poisson L, et al. (2018) Machine Learning Identifies Stemness Features Associated with Oncogenic Dedifferentiation. *Cell* 173:338-354.e15.
- Mabuchi S, Yokoi E, Komura N, Kimura T (2018) Myeloid-derived suppressor cells and their role in gynecological malignancies. *Tumour Biol* 40:1010428318776485.
- Uddin A, Chakraborty S (2018) Role of miRNAs in lung cancer. *J Cell Physiol* 20.
- Matulonis UA, Sood AK, Fallowfield L, Howitt BE, Sehouli J, et al. (2016) Ovarian cancer. *Nat Rev Dis Primers* 2:16061.
- Mahmood RD, Morgan RD, Edmondson RJ, Clamp AR, Jayson GC (2020) First-Line Management of Advanced High-Grade Serous Ovarian Cancer. *Curr Oncol Rep* 22:64.
- Bast RC Jr, Hennessy B, Mills GB (2009) The biology of ovarian cancer: new opportunities for translation. *Nat Rev Cancer* 9:415-28.
- Jones HM, Fang Z, Sun W, Clark LH, Stine JE, et al. (2017) Atorvastatin

- exhibits anti-tumorigenic and anti-metastatic effects in ovarian cancer *in vitro*. *Am J Cancer Res* 7:2478-2490.
12. Duffy MJ, Bonfrer JM, Kulpa J, Rustin GJ, Soletormos G, et al. (2005) CA125 in ovarian cancer: European Group on Tumor Markers guidelines for clinical use. *Int J Gynecol Cancer* 15:679-91.
 13. Huang S, Sun C, Hou Y, Tang Y, Zhu Z, et al. (2018) A comprehensive bioinformatics analysis on multiple Gene Expression Omnibus datasets of nonalcoholic fatty liver disease and nonalcoholic steatohepatitis. *Sci Rep* 8:7630.
 14. Petryszak R, Burdett T, Fiorelli B, Fonseca NA, Gonzalez-Porta M, et al. (2014) Expression Atlas update--a database of gene and transcript expression from microarray- and sequencing-based functional genomics experiments. *Nucleic Acids Res* 42:D926-32.
 15. Gao L, Ying F, Cai J, Peng M, Xiao M, et al. (2023) Identification and validation of pyroptosis-related gene landscape in prognosis and immunotherapy of ovarian cancer. *J Ovarian Res* 16:27.
 16. Pfeffer SR (2017) Rab GTPases: master regulators that establish the secretory and endocytic pathways. *Mol Biol Cell* 28:712-715.
 17. Vieira OV (2018) Rab3a and Rab10 are regulators of lysosome exocytosis and plasma membrane repair. *Small GTPases* 9:349-351.
 18. de Bruijn DR, dos Santos NR, Kater-Baats E, Thijssen J, van den Berk L, et al. (2002) The cancer-related protein SSX2 interacts with the human homologue of a Ras-like GTPase interactor, *RAB3IP*, and a novel nuclear protein, SSX2IP. *Genes Chromosomes Cancer* 34:285-98.
 19. Chen L, Zhou WB, Zhao Y, Liu XA, Ding Q, et al. (2012) Cancer/testis antigen SSX2 enhances invasiveness in MCF-7 cells by repressing ER α signaling. *Int J Oncol* 40:1986-94.